

REPORT DOCUMENTATION PAGE				Form Approved OMB No. 0704-0188	
Public reporting burden for this collection of information is estimated to average 1 hour per response, including the time for reviewing instructions, searching existing data sources, gathering and maintaining the data needed, and completing and reviewing the collection of information. Send comments regarding this burden estimate or any other aspect of this collection of information, including suggestions for reducing the burden, to Department of Defense, Washington Headquarters Services, Directorate for Information Operations and Reports (0704-0188), 1215 Jefferson Davis Highway, Suite 1204, Arlington, VA 22202-4302. Respondents should be aware that notwithstanding any other provision of law, no person shall be subject to any penalty for failing to comply with a collection of information if it does not display a currently valid OMB control number. PLEASE DO NOT RETURN YOUR FORM TO THE ABOVE ADDRESS.					
1. REPORT DATE (DD-MM-YYYY) 25-10-2006		2. REPORT TYPE Final Report		3. DATES COVERED (From – To) 31 August 2006 - 28-Feb-07	
4. TITLE AND SUBTITLE Testing of UHTC Samples in the VKI Plasmatron			5a. CONTRACT NUMBER FA8655-06-1-3078		
			5b. GRANT NUMBER		
			5c. PROGRAM ELEMENT NUMBER		
6. AUTHOR(S) Professor Douglas G Fletcher			5d. PROJECT NUMBER		
			5d. TASK NUMBER		
			5e. WORK UNIT NUMBER		
7. PERFORMING ORGANIZATION NAME(S) AND ADDRESS(ES) Von Karman Institute for Fluid Dynamics (VKI) Ch. De Waterloo, 72 Rhode-St-Genèse 1640 Belgium				8. PERFORMING ORGANIZATION REPORT NUMBER N/A	
9. SPONSORING/MONITORING AGENCY NAME(S) AND ADDRESS(ES) EOARD PSC 821 BOX 14 FPO AE 09421-0014				10. SPONSOR/MONITOR'S ACRONYM(S)	
				11. SPONSOR/MONITOR'S REPORT NUMBER(S) Grant 06-3078	
12. DISTRIBUTION/AVAILABILITY STATEMENT Approved for public release; distribution is unlimited.					
13. SUPPLEMENTARY NOTES					
14. ABSTRACT This report results from a contract tasking Von Karman Institute for Fluid Dynamics (VKI) as follows: The proposed activity involves testing of Ultra-High Temperature Ceramic (UHTC) material samples in the VKI Plasmatron, which is an Inductively-Coupled Plasma (ICP) facility. ICP facilities are electrodeless, so the plasma stream produced for material testing and characterization is of very high purity. The VKI Plasmatron has the largest installed power capability of this type of facility in the world. Test conditions are chosen such that the supersonic atmospheric (re-)entry boundary layer test conditions are replicated in the subsonic flow of the ICP stream. Total enthalpy, pitot pressure, and velocity gradient are the important parameters that are matched to ensure the test condition fidelity. Test condition requirements for the UHTC sample tests are heat flux of approximately 4 MW/m2, pressure of 5000 Pa, and surface temperatures on the order of 1800 C or greater. The actual conditions will be determined using a spare sample to verify the surface temperature. A pitot probe will be used to set the pressure condition and a water-cooled calorimetric probe will be used to measure the fully catalytic cold-wall heat flux, which will be used as the reference heat flux condition for the tests. The supplier of the samples for testing, and the PI for the investigation is Dr. Jochen Marschall of SRI.					
15. SUBJECT TERMS EOARD, ceramic , ultra high temperature ceramics					
16. SECURITY CLASSIFICATION OF:			17. LIMITATION OF ABSTRACT UL	18. NUMBER OF PAGES 22	19a. NAME OF RESPONSIBLE PERSON KEVIN J LAROCHELLE, Maj, USAF
a. REPORT UNCLAS	b. ABSTRACT UNCLAS	c. THIS PAGE UNCLAS			19b. TELEPHONE NUMBER <i>(Include area code)</i> +44 (0)20 7514 3154

**von Karman Institute for Fluid Dynamics
Aeronautics / Aerospace Department**

Chaussée de Waterloo, 72
B - 1640 Rhode Saint Genèse
Belgium


Contract Report: CR2006-27


Internal Ref.: 06/VKI/AR/DF/ARR0615

Testing of UHTC Samples in the VKI Plasmatron



von Karman Institute for Fluid Dynamics

 Von Karman Institute for Fluid Dynamics		CLASSIFICATION			CATEGORY		
		1. Unclassified <input type="checkbox"/> 2. Industry <input checked="" type="checkbox"/> 3. Restricted <input type="checkbox"/> 4. Confidential <input type="checkbox"/>			1. For approval <input type="checkbox"/> 2. For review <input type="checkbox"/> 3. Other <input type="checkbox"/>		
		CONFIGURATION					
Controlled				Not Controlled			
Program number	Program	Contract number		Work package number			
EOARD		AFOSR/EOARD Grant 063078		1			
TITLE: <p style="text-align: center;">Testing of UHTC Samples in the VKI Plasmatron</p>							
AUTHOR(S): <p style="text-align: center;">C. Asma, J. Thoemel, P. Collin, D. Fletcher</p>							
ISSUE. Date: July, 2006 Issue 1 Rev. 0.		Internal Reference Number 06/VKI/AR/DF/ARR0615		Number of pages: 19 Number of included annexes: 0			
SUMMARY: This technical report presents the UHTC sample tests carried out in the VKI Plasmatron. The methodology for catalycity determination is applied for the specified condition on the UHTC samples.							
HOST SYSTEM	HARDWARE EQUIPMENT. Nature: PC	MEDIA. Nature & Type: Identification:		SOFTWARE. Name: Microsoft Word			
KEY WORDS		LANGUAGE CODE ENG		APPROVAL.			
				Section: High Speed Aerodynamics			
				Department: Aeronautics/Aerospace			

 <p>Von Karman Institute for Fluid Dynamics</p>		<p>DOCUMENT REVISIONS TRACEABILITY SHEET</p> <p>DOCUMENT 06/VKI/AR/DF/ARR0615</p>	
Version	Date:	Status:	No. of pages:
Title: Author: Features:			
Version	Date:	Status:	No. of pages:
Title: Author: Features:			
Version	Date:	Status:	No. of pages:
Title: Author: Features:			

<u>1</u>	<u>ACKNOWLEDGEMENT</u>	<u>5</u>
<u>2</u>	<u>DISCLAIMER</u>	<u>5</u>
<u>3</u>	<u>INTRODUCTION</u>	<u>6</u>
<u>4</u>	<u>EXPERIMENTAL SETUP.....</u>	<u>6</u>
4.1	FACILITY.....	6
4.2	INSTRUMENTATION	7
4.2.1	HEAT FLUX PROBE.....	7
4.2.2	SAMPLE HOLDER	8
4.2.3	PYROMETER.....	9
4.2.4	INFRARED CAMERA	10
4.2.5	LIF DIAGNOSTICS	10
<u>5</u>	<u>TEST CONDITIONS AND FACILITY CALIBRATION.....</u>	<u>11</u>
<u>6</u>	<u>EXPERIMENTAL RESULTS</u>	<u>11</u>
<u>7</u>	<u>REBUILT RESULTS AND ABACUS PLOTTING</u>	<u>15</u>
7.1	REBUILDING RESULTS	16
<u>8</u>	<u>NUMERICAL SIMULATIONS.....</u>	<u>17</u>
8.1	ICP SIMULATION.....	18
8.2	BOUNDARY LAYER PROPERTIES	18
8.3	FILES DELIVERED WITH THE REPORT	20
<u>9</u>	<u>CONCLUSION</u>	<u>20</u>
<u>10</u>	<u>REFERENCES</u>	<u>21</u>

1 Acknowledgement

- This effort is sponsored by the Air Force Office of Scientific Research, Air Force Material Command, USAF, under grant number FA8655-06-1-3078. The U.S. Government is authorized to reproduce and distribute reprints for Government purpose notwithstanding any copyright notation thereon.

2 Disclaimer

- The views and conclusions contained herein are those of the author and should not be interpreted as necessarily representing the official policies or endorsements, either expressed or implied, of the Air Force Office of Scientific Research or the U.S. Government.
- We certify that there were no subject inventions to declare during the performance of this grant.

3 INTRODUCTION

This report summarizes the work performed at von Karman Institute to test the UHTC samples in the VKI Plasmatron Facility. A DVD attached to this report completes the information given in this report.

4 EXPERIMENTAL SETUP

4.1 Facility

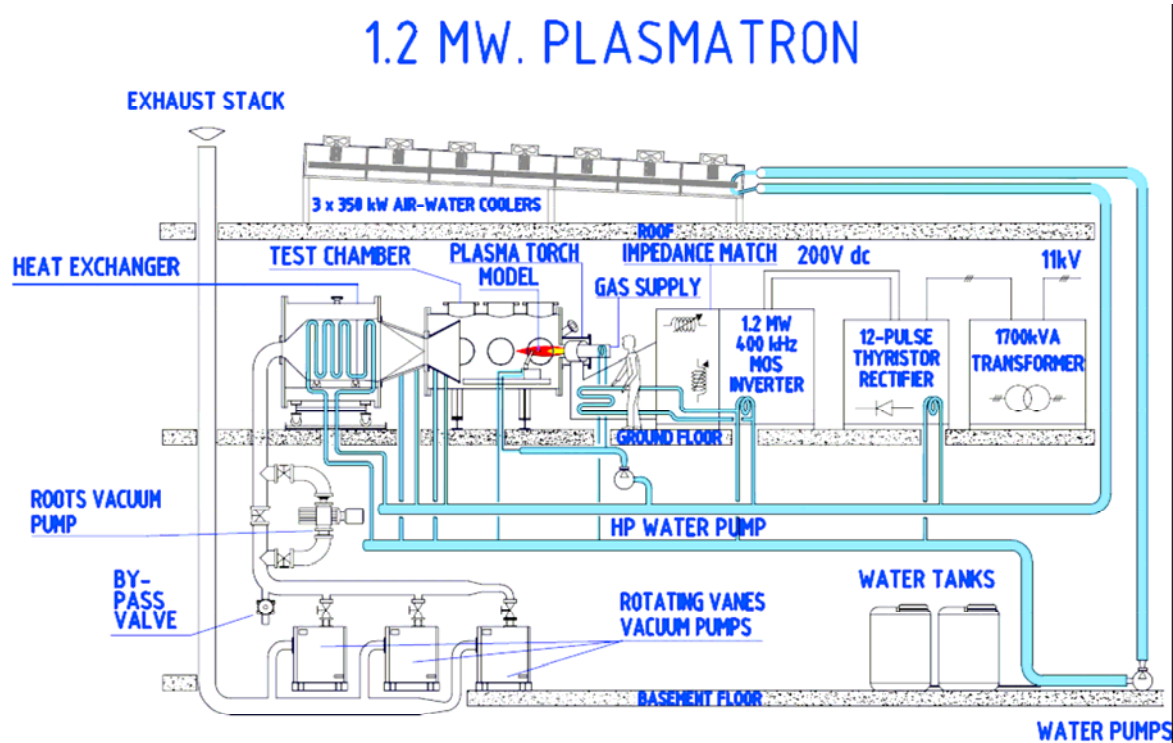


Figure 1: The VKI Plasmatron Facility

The complete VKI Plasmatron Facility [1], [2], [3] is sketched in Fig. 1. It is configured with an ICP torch, of 160 mm diameter suited for material testing. The torch is mounted inside a support enclosure, which is fixed on a side of the test chamber. The test chamber is a 2.5 m long, 1.4 m diameter vessel equipped with multiple portholes and windows to allow maximal flexibility and unrestrained optical access for plasma diagnostic techniques. Inside the enclosure, the samples and probes are mounted on a fast-injection system.

The plasma jet is collected at the outlet of the enclosure and cooled in the heat exchanger to a maximum temperature of 50°C to protect the vacuum plant from overheating damage. The vacuum plant consists of three volumetric vacuum pumps, which allow operating pressures between 1 hPa and atmospheric pressure with a maximum flow rate of 3000 m³/h. A Roots pump can be inserted in the circuit to achieve lower operating pressures. Exhaust gases are then vented to the atmosphere through a stack.

The Plasmatron is equipped with a 1.2 MW, 400 kHz, high-frequency generator of relatively new solid-state technology, using thyristors and MOS inverters instead of vacuum tubes. An extensive closed circuit cooling system using de-ionised water protects all facility parts from melting due to the plasma heat, which is dissipated through three dry air coolers located on the roof of the installation. For air plasma operation, the facility is connected to the VKI compressed air supply.

4.2 Instrumentation

4.2.1 Heat Flux Probe

This probe (Fig. 2) is made mainly of copper and its external shape is the same as the sample holder to conserve all the parameters of similitude (dynamic pressure, stagnation heat flux and velocity gradient). The walls are cooled by water and a calorimeter described in the next part is placed in the centre of the front face. The heat flux values are determined from the water-cooled calorimeter as described in section 4.2.1.1.

In a plasma heating experiment, there are three possible contributions to heat flux for a test sample placed in the stagnation point configuration. These are convective, chemical (surface-catalyzed recombination) and radiative heating. Note that the calorimeter has a polished copper surface, which is intended to improve the sensitivity to chemical heat flux rather than radiative heat flux.

Note that the heat flux is measured on a cold wall made of copper, which is considered to be fully catalytic for any plasma (air or CO₂), and it is polished before each application to give a reference status for the surface.

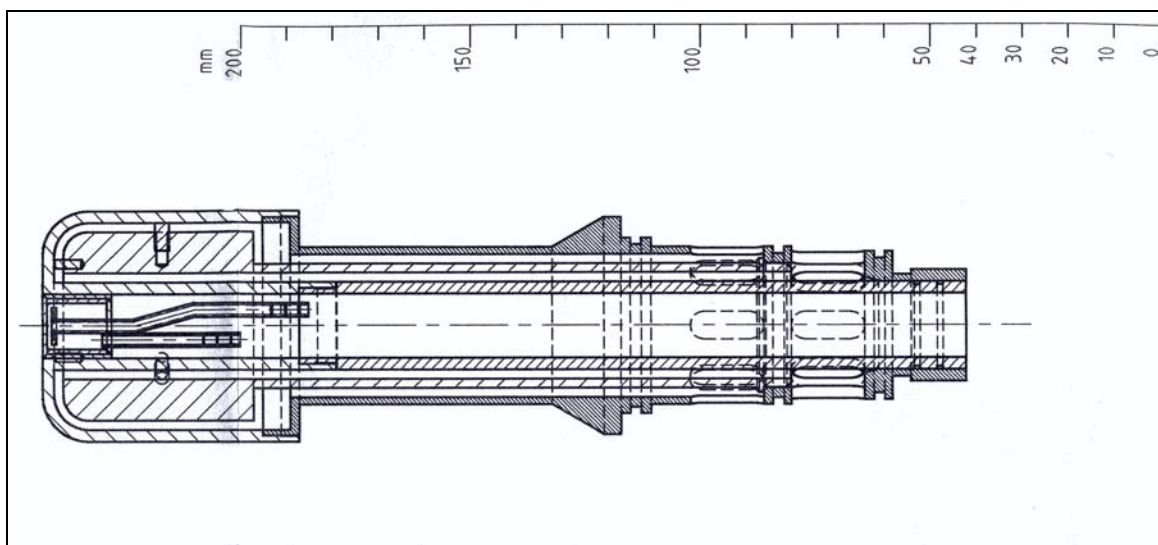


Figure 2: Sketch of the heat flux probe, with water-cooled calorimeter installed inside

4.2.1.1 Copper Water-Cooled Calorimeter

The calorimeter is used to measure the heat flux at the stagnation point of the heat flux probe (Figure 3). It measures the fully catalytic heat flux on a cold wall ($\approx 300\text{K}$) by measuring the mass flow and the temperature difference in the cooling water supply and return lines.

The water temperature is measured in the inlet and the outlet of the calorimeter by using two type K thermocouples and the mass flow of the cooling water is controlled by a rotameter and is measured before every test. In order to have correct measurement, the sidewalls of the calorimeter have to be adiabatic. An insulator is installed between the calorimeter and the wall of the probe for this purpose. Then the heat flux is given by:

$$\dot{q} = \frac{\dot{m}C_p(T_{out} - T_{in})}{S}$$

where

\dot{m} : mass flow in the calorimeter [kg/s]

C_p : heat capacity of water [J/kg.K]

T_{out} : temperature at the outlet of the calorimeter [K]

T_{in} : temperature at the inlet of the calorimeter [K]

S : front surface area of the calorimeter [m^2]

A large number of tests have been carried out with this calorimeter at VKI, and it has proven to be both robust and reliable.

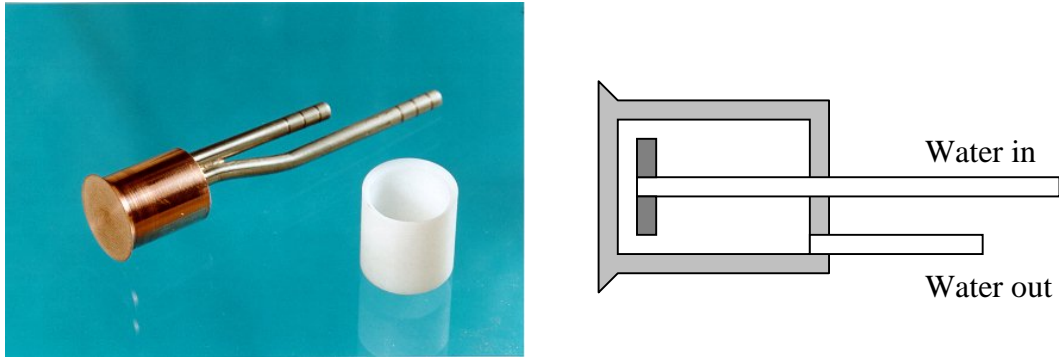


Figure 3: Water-cooled calorimeter

4.2.2 Sample Holder

The Sample holder (Fig. 4) is composed of two coaxial tubes in which water circulates for cooling. At the extremity, a support for the sample made of SiC (Fig. 5) is attached to the holder body by three metallic pins. The sample is installed in this support and held with a second set of three pins. An insulator (kapirok) is placed between the sample and the sample holder.

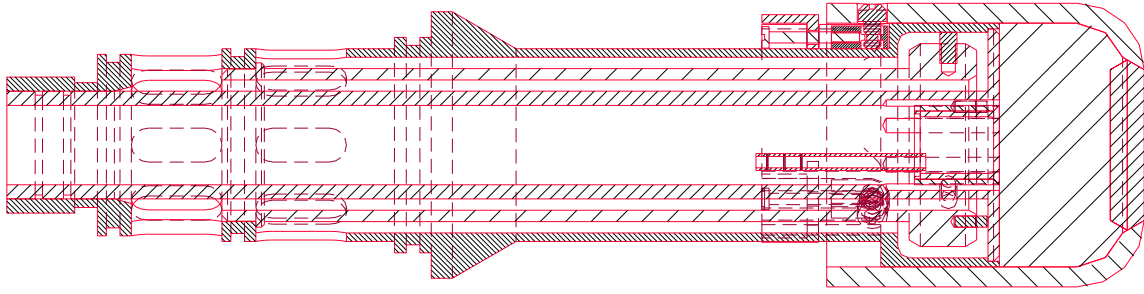


Figure 4: Sample holder

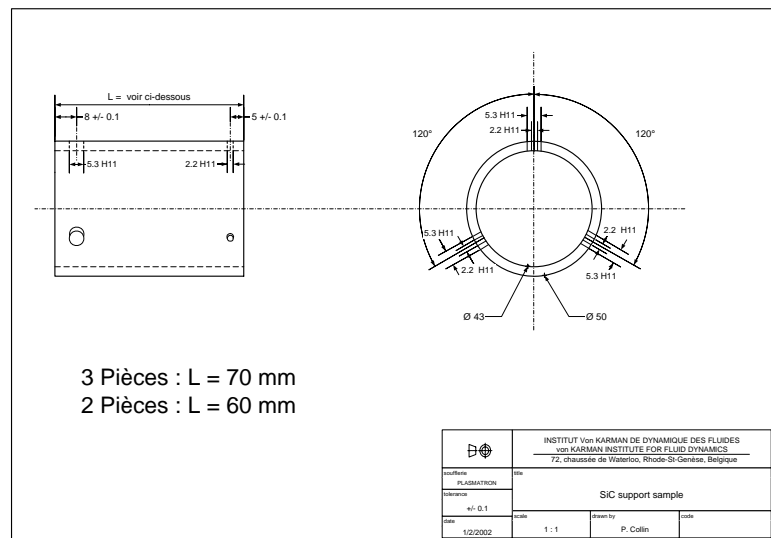


Figure 5: Support of sample

4.2.3 Pyrometer

A two-color pyrometer (Raytek Marathon Series MR1SC, Serial #: 46667, Lot #: 2360430101, Temperature Range: 1000-3000°C) is used to measure the surface temperature of the sample during the test. This device measures the IR emission from the surface at two different wavelengths that are fairly close to each other. If the emissivity, ϵ , of the material is considered constant over the two wavelengths an absolute temperature measurement can be determined from a Planck's law analysis for a grey gas. The acquisition speed is 1 Hz. The wavelength range of the pyrometers is 0.8 to 1.1 microns for the first detector (used for one colour measurement) and 1.0 to 1.1 microns for the second detector.

The pyrometer is calibrated using a black-body radiation source to take into account the effect of the window. The resulting calibration-curve is as follows, with an uncertainty of $\pm 10^\circ\text{C}$:

$$T_{\text{real}}[\text{C}] = 0.887T_{\text{pyrometer}}[\text{C}] + 65.687$$

The angle between the sample and the pyrometer is 20 degrees in horizontal plane (Angle 'b' in Fig. 6) and 22 degrees in vertical plane (Angle 'a' in Fig. 6).

4.2.4 Infrared Camera

A FLIR infrared camera is used at the range of 500C ~ 1300C to record the surface temperature of the samples. A Zn-Se window installed at Plasmatron wall allows the infrared radiation to pass. The infrared camera is not calibrated and the results are emissivity dependant. The wavelength range of the infrared camera is 8 to 9 microns.

The angle between the sample and the infrared camera is 26 degrees in horizontal plane (Angle 'b' in Fig. 6) and 33 degrees in vertical plane (Angle 'a' in Fig. 6).

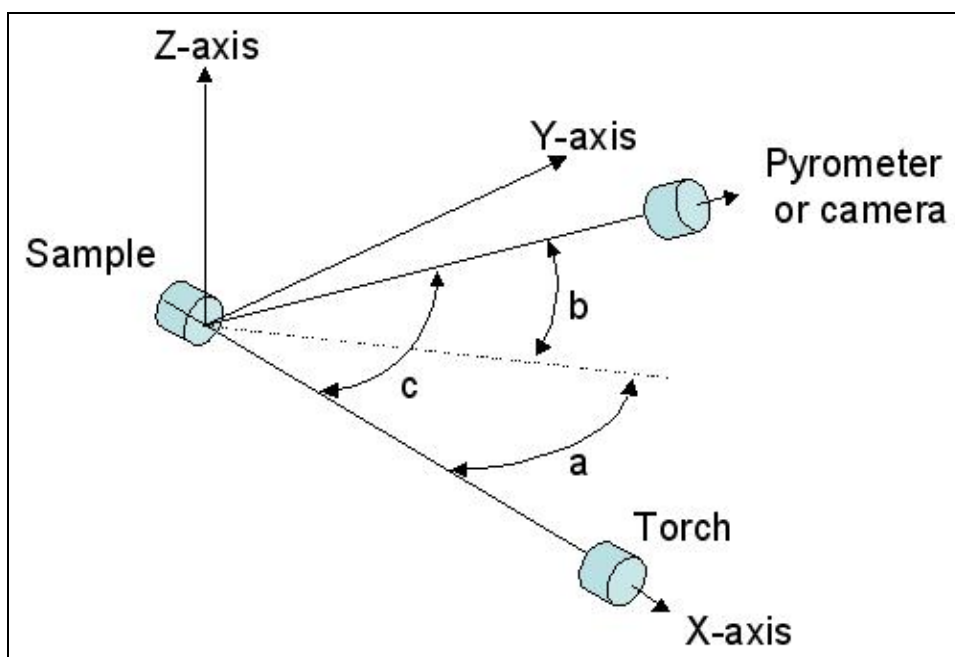


Figure 6: Angles between the detectors and the sample

4.2.5 LIF Diagnostics

Early in the development of plasma wind tunnels for aerospace material testing and development, attempts were made to diagnose the plasma state using emission spectroscopy. Applications of emission spectroscopy continue in plasma facilities, however, its implementation and the subsequent interpretation of the spectral intensities in terms of thermodynamic and chemical parameters of the plasma has not been universally successful. A number of applications have demonstrated the need for acquiring radial profile measurements, owing to the influence of thermal and chemical gradients along the line of sight. To overcome this limitation, a number of research groups have applied spatially resolved spectroscopic techniques to characterize plasma flows over a wide range of flow speeds and test gases. Laser-induced-fluorescence (LIF) is one such approach that has shown promising results in a number of plasma flow characterization applications. LIF produces spatially resolved measurement at the location of the intersection of the laser beam and the fluorescence detection optical system. Furthermore, since fluorescence is used to monitor the excitation process, the information about a particular flow species obtained from the LIF signals is representative of the ground electronic state population rather than an excited state population, which may not be in Boltzmann equilibrium with the ground state. For applications involving air plasmas, typical target species include NO, N and O [9].

5 TEST CONDITIONS AND FACILITY CALIBRATION

The purpose of the test campaign is to keep the samples under plasma flow at steady state conditions based on facility power and sample front face temperature. Some initial tests are performed using the same sample to see which power corresponds to which surface temperature and also to detect the problems, if any.

Three different samples are used for this purpose, which are samples no 17, 18 and 19. All tests are performed at 50mbar static pressure conditions. Sample 17 is exposed to air plasma flow at a mass flow rate of 16 g/s and at a power level varying between 150kW and 200kW. The surface temperature values have varied between 1260C and 1400C. The same sample is afterwards exposed to a plasma flow of 8g/s mass flow rate at similar power conditions, however the SiC cover is broken during these tests. The trials with the other samples (no 18 and 19) resulted similarly; the SiC cover is broken eventually although a steady state front face temperature of 1460C is observed at 175kW power. Sample 19 is also tested with a longer SiC cover and at higher pressure (100mbar) and higher mass flow rate (16g/s). The SiC cover is not broken during this test.

The results of the calibration phase forced us to change the conditions. For the actual tests, the following conditions are respected:

- A longer SiC cover is used
- The static pressure is set to 100mbar
- Mass flow rate of air is set to 16g/s
- Samples are injected at low power (~110kW) and the power is increased slowly to its target value in ~1 minute.
- The power is decreased slowly at the end of the test to ~100kW, till the surface temperature decreases below 1000C.

6 EXPERIMENTAL RESULTS

Table 1 presents a summary of all the tests performed. As a precaution, the first tests are started at lower power (150kW) and the power is increased as the tests are successful. Some conditions are repeated by changing the total duration, where the purpose is to see the effect of duration. No significant mass change has been observed for any of the samples tested.

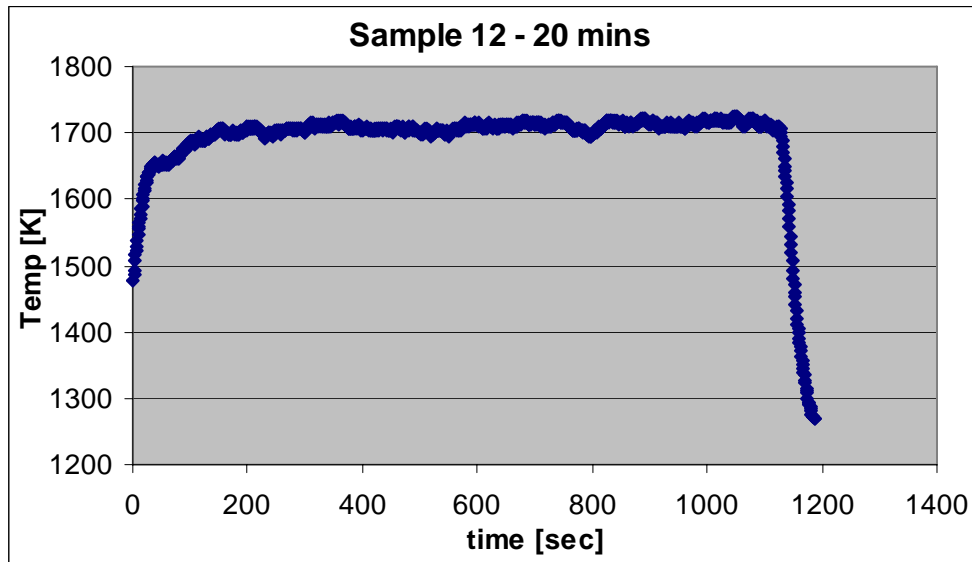
The heat flux is determined by a water-cooled calorimeter and the surface temperature is determined by the two-colour pyrometer. The temperature values given in Table 1 are already calibrated values. All the tests are carried out without any problems except for the last test (Test no 16, Sample 4), where the Plasmatron facility has stopped after 15 minutes of testing. Since the purpose of this test was to keep the sample in plasma flow for 20 minutes, the facility is restarted and the sample is kept under plasma flow for another 5 minutes.

Table 1 Summary of Tested Samples

Test no	Sample	Date	Time	p_stat [mbar]	Power [kW]	H. Flux [kW/m ²]	p_dyn [Pa]	Duration	Tsteady [C]
5	20	31/5/2006	14:30	100	150	510	24	10 mins	1241
6	16	31/5/2006	16:00	100	160	715	25	10 mins	1387
7	15	1/6/2006	10:05	100	160	730	26	5 mins	1356
8	14	1/6/2006	11:25	100	160	755	26	20 mins	1387
9	13	1/6/2006	14:00	100	170	905	28	10 mins	1458
10	12	1/6/2006	15:35	100	170	875	27	20 mins	1436
11	11	2/6/2006	11:00	100	170	900	27	5 mins	1456
12	5	6/6/2006	15:45	100	160	710	24	16 mins	1352
13	6	7/6/2006	11:15	100	190	1095	31	20 mins	1512
14	10	7/6/2006	14:25	100	190	1050	31	10 mins	1503
15	9	7/6/2006	16:05	100	210	1225	38	10 mins	1574
16	4	8/6/2006	12:05	100	210	1165	39	15+5 mins	1547

The temperature evolution of samples 12 and 6 (tests 10 and 13) are presented as examples in Figures 7 and 8, respectively. As it can be seen, the maximum fluctuations in temperature are in the order of $\pm 15\text{K}$. As an example of repeatability, the temperature evolution of sample 4 (Test 16) is presented in Figure 9. The Plasmatron had stopped after 15 minutes of testing of this sample, and then it was restarted for an additional 5 minutes. In Figure 9, it can be observed that the steady state temperature reaches to its original value after the sample cools down and the Plasmatron is restarted.

Similar plots for all the samples tested can be found in the DVD attached to this report.

*Figure 7. Temperature Evolution, Test 10, 170kW power*

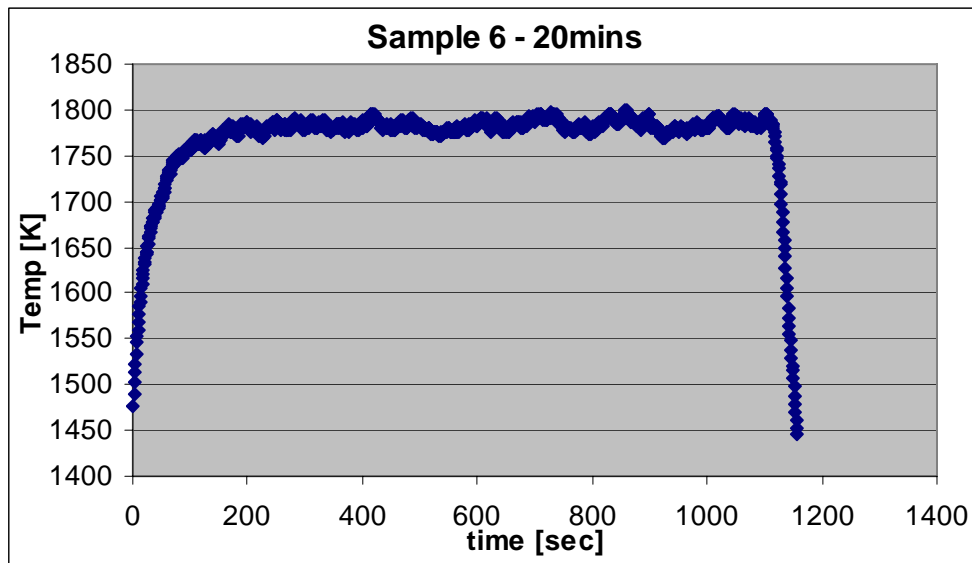


Figure 8. Temperature Evolution, Test 13, 190kW power

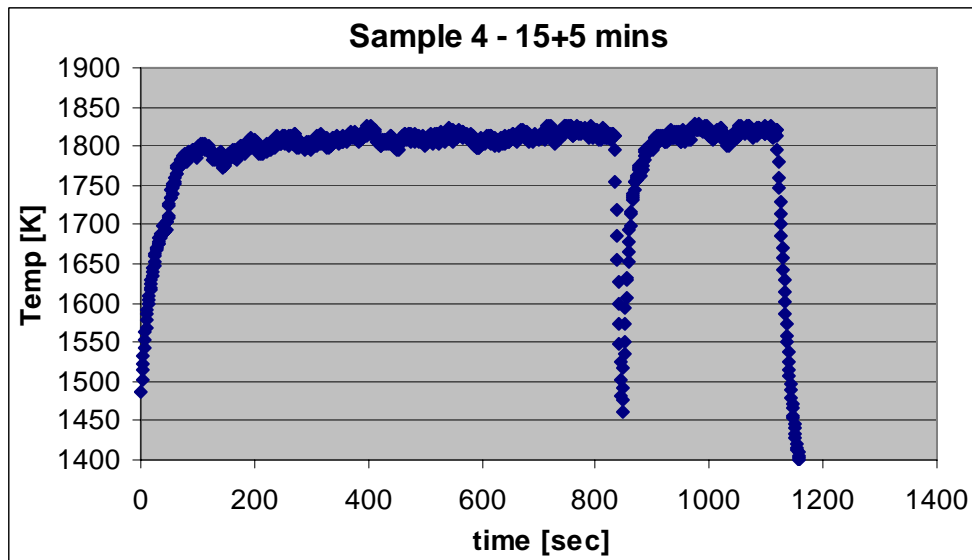


Figure 9. Temperature Evolution, Test 16, 210kW power

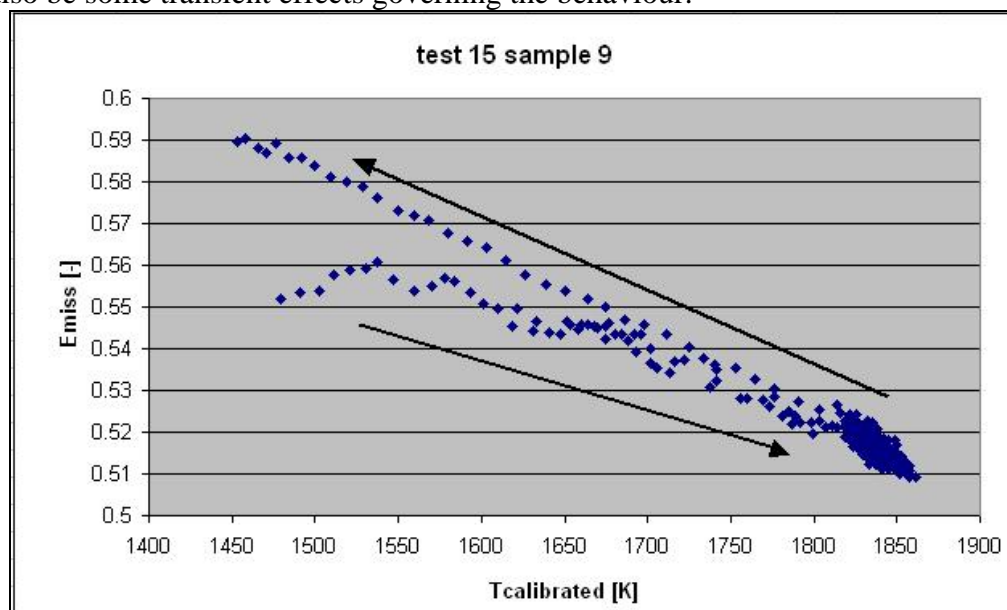
The infrared camera is employed during the tests 13, 14 and 15 (Samples 6, 10 and 9) in addition to the pyrometer. The purpose of using the infrared camera is to detect if the emissivity is changing in time. For this purpose, measurements are taken every two minutes and a “representative emissivity value” is obtained from the software of the infrared camera such that the infrared camera temperature value is equal to the two-colour pyrometer temperature value. It should be noted that this emissivity value should not be taken as the absolute emissivity value of the material. The results are presented in Table 2. A slight increase in emissivity can be observed at the beginning of the test, but then the emissivities of the materials remain constant.

During testing, green emission is observed from samples once surface temperature has reached a high value. Emission gradually disappears, and it is thought to be an oxide of Boron.

Table 2 Summary of Emissivity Evolution

Test no	Sample	Power [kW]	Time [min]	Tpyrom [C]	Tcalib [C]	Emiss [-]
13	6	190	3	1600	1484.89	0.73
13	6	190	5	1620	1502.6	0.74
13	6	190	7	1625	1507.1	0.75
13	6	190	9	1630	1511.5	0.75
13	6	190	11	1625	1507.1	0.75
13	6	190	13	1635	1515.9	0.75
13	6	190	15	1630	1511.5	0.76
13	6	190	17	1620	1502.6	0.76
13	6	190	19	1635	1515.9	0.76
14	10	190	3	1620	1502.6	0.73
14	10	190	5	1620	1502.6	0.74
14	10	190	7	1620	1502.6	0.74
14	10	190	9	1625	1507.1	0.74
15	9	210	3	1685	1560.3	0.73
15	9	210	5	1690	1564.7	0.74
15	9	210	7	1675	1551.4	0.75
15	9	210	9	1695	1569.2	0.75

A similar calculation is done using the one-colour and two-colour values of the pyrometer. Assuming that the measured intensity is proportional to the “representative emissivity” and the fourth order of the temperature, the fourth root of the ratio of one to two-colour temperature values are evaluated. A typical result is shown in Fig. 10 for sample 9 (Test 15). This plot is the calculated emissivity value vs front face temperature. The arrows indicate the evolution of time. Initial data show an emissivity value of 0.55 at ~1500K at the beginning of the test. As the time passes the temperature increases to 1850K and at the very end of the test, the temperature decreases back to 1500K. But at this moment, the emissivity is calculated to be 0.59, which is higher than the initial value. So, according to this plot, the emissivity value is higher at the end of the test for the same front face temperature. However, these results should be interpreted with care as there might also be some transient effects governing the behaviour.

*Figure 10. Emissivity vs Temperature, from pyrometry results*

7 REBUILT RESULTS AND ABACUS PLOTTING

A quick explanation about the catalycity determination is given here, more details could be found in the references [5 - 8].

The VKI Boundary Layer Code (P. Barbante, Ref [4]) provides the computation of the heat flux at the stagnation point for defined conditions of pressure (p_e) and temperature (T_e) at the outer edge, catalycities γ_i and temperature at the wall, T_w .

The functional dependence can be expressed as :

$$q_w = q_w(p_e, T_e, T_w, \delta, \frac{du_e}{dx}, \frac{\partial}{\partial y}(\frac{\partial u}{\partial x})|_e, V_e, \gamma_i)$$

This system can be solved when the values for the recombination probabilities, γ_i of the material in a defined gas mixture are known: the assumption of fully catalytic material (copper) and the use of an effective recombination probability for air give $\gamma_w = 1$.

The Rebuilding Code (ref. [7]), implemented in Fortran 90, uses an iterative procedure to solve this system: experimental and numerical fully catalytic cold wall heat fluxes are matched by iterating on the variables T_e (which determine H_e) and V_e . H_e and V_e are respectively the enthalpy and the velocity at the edge of the boundary layer. The important features and assumptions of this Rebuilding Code are given in ref. [7,8], but the most important assumption is that the edge conditions are local thermodynamic equilibrium.

The global methodology for the enthalpy rebuilding is sketched in Fig. 11. Besides the four parameters coming from the ICP Code, four other experimental (and geometrical) parameters are required as input for the Rebuilding Code. During the execution, a first choice for the temperature at the boundary layer edge (and other options) is asked.

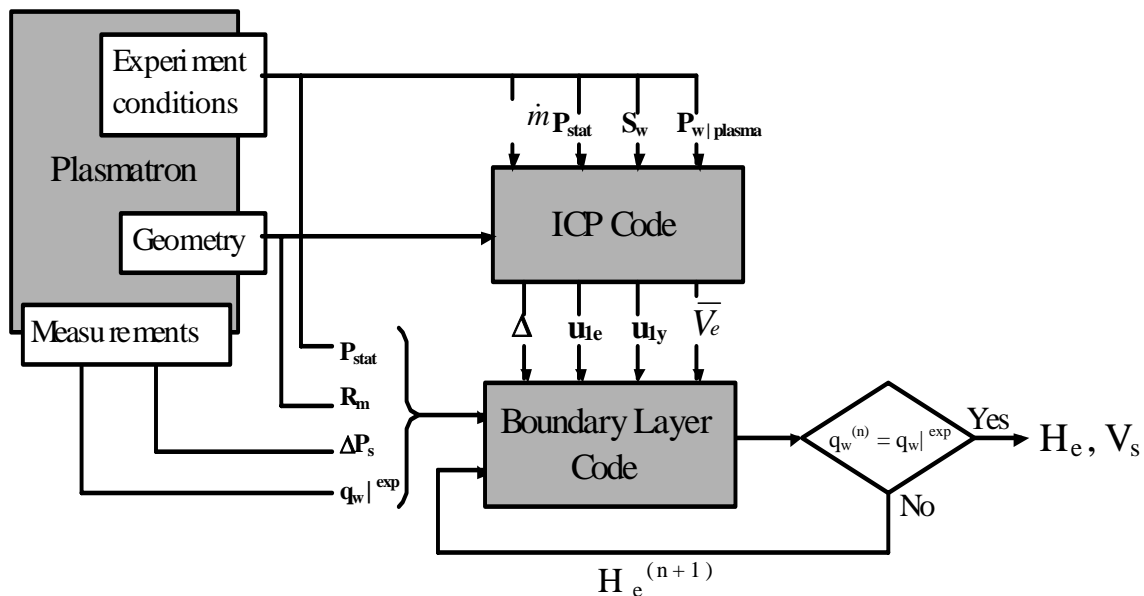


Figure 11. Enthalpy rebuilding

Note that this Rebuilding Code also takes the Barker effect into account, thus no correction is needed on the input parameter Δp_s . The Barker effect is known as the viscous effect that affects the total pressure measurements at low Reynolds number (i.e. $Re < 100$).

7.1 Rebuilding Results

Using the experimental heat flux, static pressure and dynamic pressure values (presented in Table 1), the boundary layer edge conditions have been calculated using the methodology described in the previous section. The results are given in Table 3, where total enthalpy, velocity and static temperature values at the edge of the boundary layer can be seen, as well as catalycity values. Here, Table 1 is re-presented for the sake of easiness in interpreting the results.

Table 1 Summary of Tested Samples

Test no	Sample	Date	Time	p_stat [mbar]	Power [kW]	H. Flux [kW/m ²]	p_dyn [Pa]	Duration	Tsteady [C]
5	20	31/5/2006	14:30	100	150	510	24	10 mins	1241
6	16	31/5/2006	16:00	100	160	715	25	10 mins	1387
7	15	1/6/2006	10:05	100	160	730	26	5 mins	1356
8	14	1/6/2006	11:25	100	160	755	26	20 mins	1387
9	13	1/6/2006	14:00	100	170	905	28	10 mins	1458
10	12	1/6/2006	15:35	100	170	875	27	20 mins	1436
11	11	2/6/2006	11:00	100	170	900	27	5 mins	1456
12	5	6/6/2006	15:45	100	160	710	24	16 mins	1352
13	6	7/6/2006	11:15	100	190	1095	31	20 mins	1512
14	10	7/6/2006	14:25	100	190	1050	31	10 mins	1503
15	9	7/6/2006	16:05	100	210	1225	38	10 mins	1574
16	4	8/6/2006	12:05	100	210	1165	39	15+5 mins	1547

Table 3 Summary of Rebuilding Results

Test no	Sample	Tsteady [C]	Qrad [kW/m ²]	h _e [MJ/kg]	T _e [K]	V _e [m/s]	γ [-]
5	20	1241	223.522	14.92	5437.26	95.65	3.227E-04
6	16	1387	323.023	20.43	5872.92	106.76	1.351E-03
7	15	1356	299.563	20.65	5887.04	109.22	7.577E-04
8	14	1387	323.023	21.36	5932.69	110.33	1.108E-03
9	13	1458	381.929	25.15	6159.89	120.49	1.483E-03
10	12	1436	362.882	24.54	6124.02	117.38	1.256E-03
11	11	1456	380.168	25.23	6164.18	118.43	1.465E-03
12	5	1352	296.632	20.48	5876.22	104.68	7.891E-04
13	6	1512	431.860	29.85	6438.52	134.50	1.469E-03
14	10	1503	423.217	28.60	6361.95	132.43	1.533E-03
15	9	1574	495.054	31.90	6573.08	152.75	2.032E-03
16	4	1547	466.738	30.09	6463.69	151.31	1.841E-03

One of the important assumptions in the approach used for the determination of catalycity is that the polished copper calorimeter surface has $\gamma = 1$. The true value of copper catalytic efficiency is more likely to be closer to 0.1. To illustrate the sensitivity of the heat flux determination to $\gamma = 1$ or 0.1, the variation in heat flux for varying catalycity is shown in the following figure. The heat flux increases by about 2% for $\gamma = 1$, compared to $\gamma = 0.1$, and this is already within the uncertainty of the measurements.

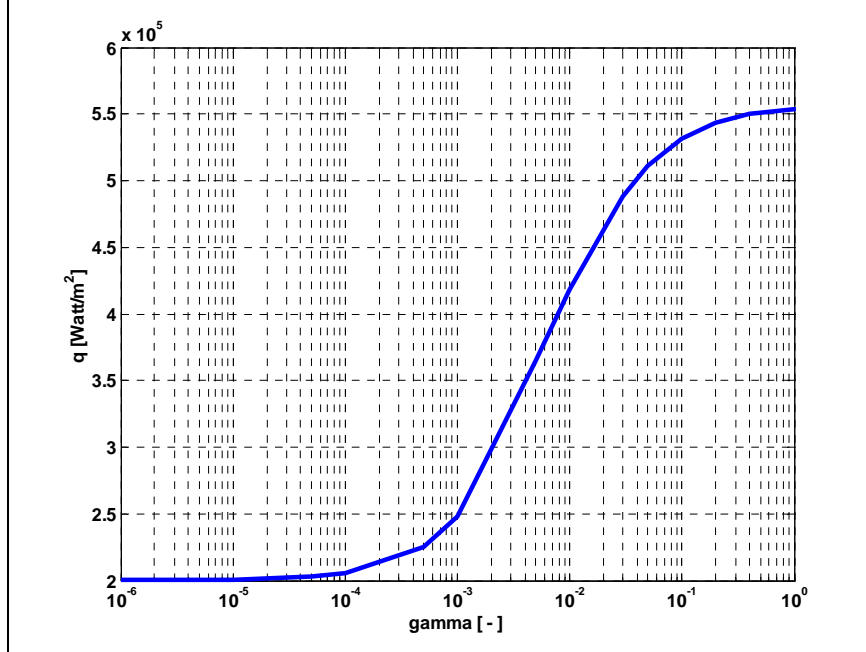


Figure 12. Heat flux as a function of surface catalycity.

8 NUMERICAL SIMULATIONS

The determination of catalytic properties of TPS materials is a major issue for the aerospace vehicles. These properties strongly affect the heat transfer to the materials with up to a factor of two greater heat flux for a fully catalytic material compared to a non-catalytic material. Knowledge of TPS catalytic properties is extremely important for designing aerospace vehicles that have very stringent mass budget, for reusable launch vehicles the problem is even more critical. Two main difficulties arise to carry out these investigations and tests. Firstly, the complete duplication of the aerothermodynamic conditions for hypersonic flight cannot be achieved in existing ground test facilities. Thus, only the local heating environment on critical parts of the spacecraft can be replicated in discharge-plasma facilities for sufficient test times to evaluate TPS material performance in real flight conditions. Secondly, the partial catalycity effects involve wall chemistry in non-equilibrium condition. This fact makes detailed measurements not easy to realize and in most of the cases the investigations lead to a global information for which a data processing is need to determine the chemical contribution to the total heat flux at the wall. For this testing, a methodology centred on Local Heat Transfer Simulation (LHTS), has been developed. It allows evaluating the catalytic properties of TPS materials based on a combination of Plasmatron tests and CFD modelling. A fully catalytic stagnation point heat flux probe and a pitot probe are used for the characterization of the plasma flow at the location of the test sample, for given Plasmatron conditions. The numerical computations of the same test configuration provided the aerodynamics parameters at the edge of the boundary layer of the sample. These two sets of result are then used as inputs data for a reacting boundary layer code which provides the heat flux abacus (heat flux at

the stagnation point versus wall temperature) with wall catalycity coefficient as a parameter. The effective catalycity coefficient of the TPS material can be determined by interpolation, in this reference abacus, plotting the stagnation point heat flux and the wall temperature obtained during the sample test measurements.

This report documents the properties of the flow field for two representative test cases.

8.1 ICP Simulation

For numerical investigations of the flow field, two experimental conditions have been chosen. Firstly those of test no. 9 and secondly those of test no 15. They are summarized as follows:

- Mass flow rate = 16g/s,
- $p_{\text{static}} = 100\text{mbar}$,
- $P_{\text{EM},9} = 170\text{kW}$ and $P_{\text{EM},15} = 210\text{kW}$.

The ambient conditions used in the simulations of the flow inside the PLASMATRON coincide with the conditions actually used in the experiments with the exception of the imposed electromagnetic power. The generator efficiency is generally assumed to be ~55%.

The simulations were carried out assuming a local thermodynamic equilibrium air model. The transport properties are computed by the help of kinetic theory and the thermodynamic properties by the use of statistical thermodynamics. The computations of both sets of properties are done by an in-house developed library called PEGASE. The air model consist of a mixture of eleven species as follows: O_2 , N_2 , NO , O , N , N^+ , O^+ , NO^+ , N_2^+ , O_2^+ , e^- .

The Non Dimensional Parameters obtained are shown in Table 4. They serve as the numerical input for the boundary layer stagnation line computation. This set is used for all boundary layer computations since it has been shown, that the impact of them onto the solution is little.

Table 4 Obtained non-dimensional-parameters (NDPs)

Δ	u_{1e}	u_{1y}	V_e
0.4596	0.2041	0.4489	0.2483

The results of the simulations are shown in Figures 1,2 and 3 in the Appendix A of the file UHTC_CFD_Report_VKI.pdf for test no. 15. The corresponding tecplot files for both cases are delivered in the CD attached to this report.

8.2 Boundary Layer Properties

The distribution of the species along the stagnation line is shown in Figures 13 and 14. Furthermore the temperature is drawn. As expected a significant amount of atomic nitrogen and especially oxygen is present at the wall.

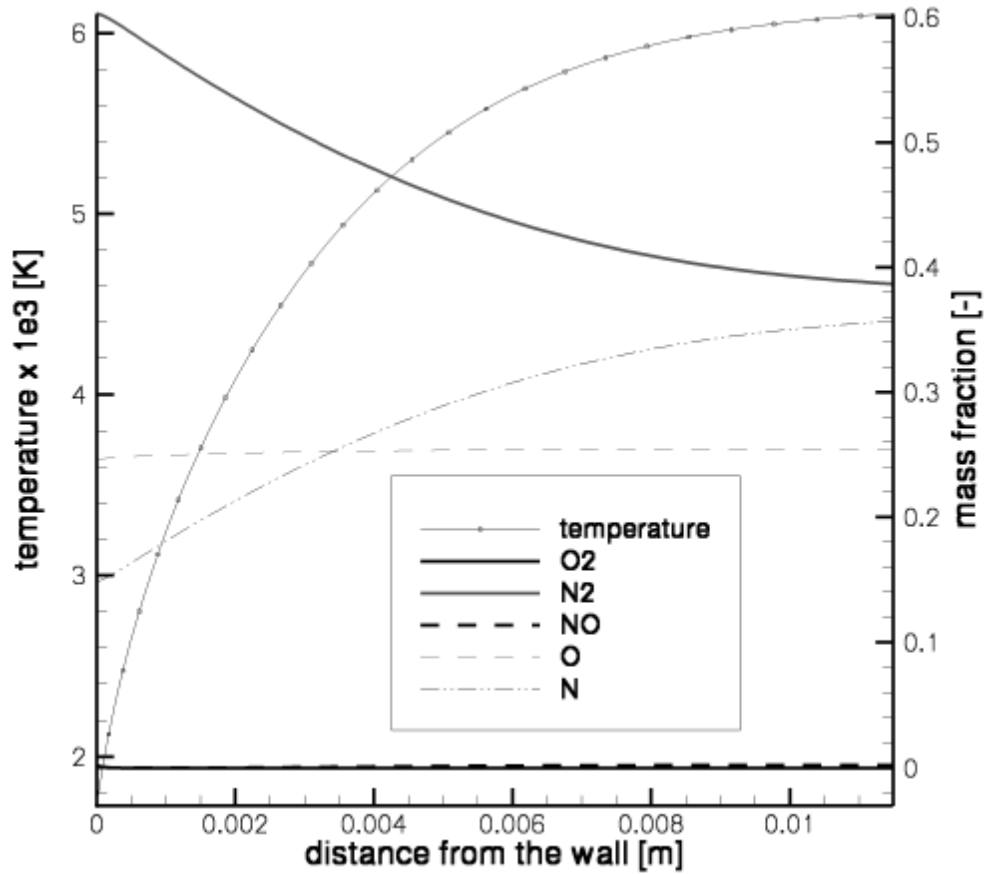


Figure 13 Temperature and mass fraction in the boundary layer; Test no 9.

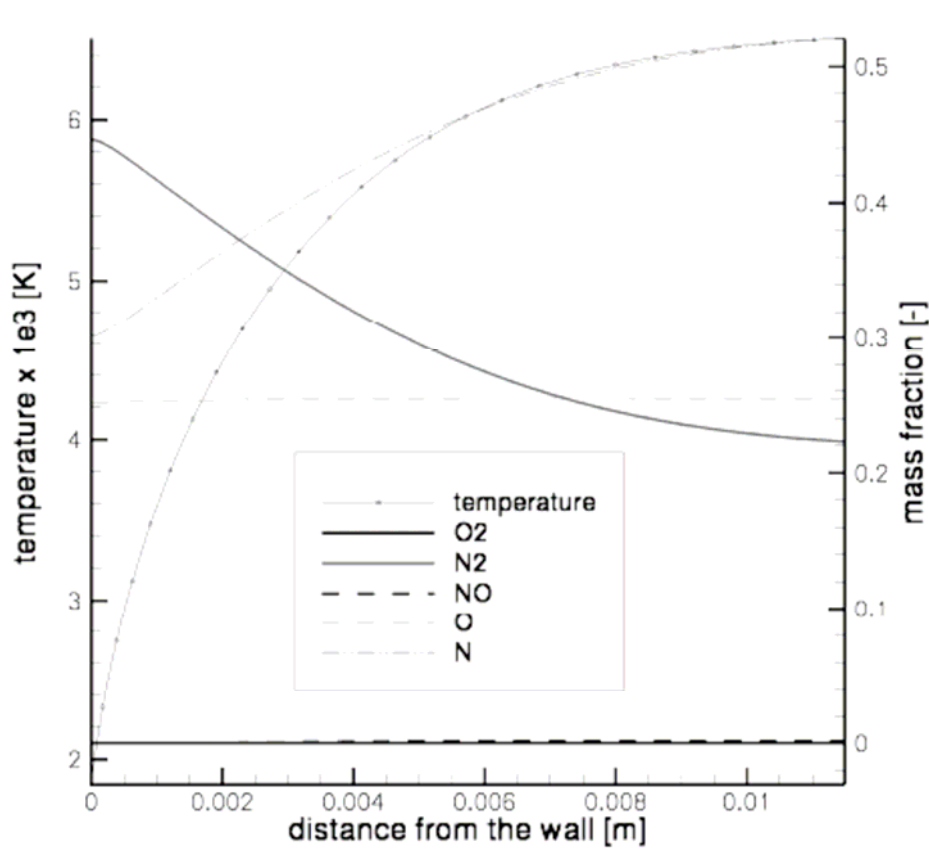


Figure 14 Temperature and mass fraction in the boundary layer; Test no 15.

To find the number densities that correspond to the species mass fractions, the following relation is used

$$n_i = \frac{\rho N_A c_i}{MW_i}$$

where n_i is the number density, N_A is Avogadro's number, c_i is the mass fraction, and MW is molecular weight of species i . If it is not explicitly given in the output files of the simulations, the density can be found by using the chamber static pressure, the computed temperature, and the gas constant for the mixture $R_m = \sum c_i R_i$.

8.3 Files Delivered with the Report

Table 5 summarizes the list of files delivered with this report.

Table 5 Overview of delivered files

name of the file	format	comment on the content
	tecplot	flow properties of PLASMATRON domain test no. 9
	tecplot	flow properties of PLASMATRON domain test no. 15
	tecplot	flow properties stagnation line test no. 9
	tecplot	flow properties stagnation line test no. 15
	Excel	overview experimental and computational results for all tests
	pdf	this report

9 CONCLUSION

The tests conducted in the VKI Plasmatron were done on UHTC samples for pressure and surface temperature conditions specified by the customers. Wall temperature, mass loss, heat flux and pressure measurements are performed during these tests and during the facility calibration. Enthalpy rebuilding is followed by catalycity determination.

LIF measurements were made for N as the target species, since 226nm mirrors were delayed (not delivered on time). Test conditions will be re-done for oxygen LIF and O species population and temperature at the edge of the boundary layer will be measured to verify CFD results.

10 REFERENCES

- [1] Mario Carbonaro, Benoit Bottin, Vincent Van Der Haegen.
Plasmatron Definition File P1-DF-1.1-VKI. July 1998
- [2] B.Bottin, M. Carbonaro, S. Paris, V.Van Der Haegen, A. Novelli, D. Vennemann
The VKI 1.2MW Plasmatron Facility for the Thermal Testing of TPS Materials.
3rd European Workshop on Thermal Protection Systems, ESTEC, Noordwijk, The Netherlands, March 25-27, 1998
- [3] B.Bottin, M. Carbonaro, V.Van Der Haegen, S. Paris
Predicted and Measured Capability of the Plasmatron Regarding Re-entry Simulation.
International Symposium on Atmospheric Reentry Vehicles and Systems, Arcachon, France, March 16-18, 1999
- [4] Gülhan, A., Esser, B., *A Study on Heat Flux Measurements in High Enthalpy Flows*,
AIAA 2001-3011, 35th AIAA Thermophysics Conference, 11-14 June 2001, Anaheim, CA, USA.
- [5] Kolesnikov, A. *Combined measurements and computations of high enthalpy and plasma flows for determination of TPM surface catalycity*. Paper presented at the RTO AVT course on "Measurement Techniques for High Enthalpy and Plasma flows". Rhode Saint Genese, October 1999. Published in RTO EN-8.
- [6] O. Chazot, M. De la Llave Plata, B. Bottin, M. Carbonaro, *The VKI inductive plasma facilities and their application to surface catalycity studies for planetary re-entry*. 93th Semiannual meeting of the supersonic Tunnel Association, 30 April – 2 May 2000, Sunnyvale, California, USA
- [7] Garcia Muñoz, A. : *Catalycity effects in plasma flows*, Diploma Project Report , VKI, June 2001.
- [8] Barbante, P.F. : *Accurate and Efficient Modelling of High Temperature Nonequilibrium Air Flows*. PhD thesis, Université Libre de Bruxelles, May 2001.
- [9] Fletcher, D. G and Playez, M., *Characterization of Supersonic and Subsonic Plasma Flows*. AIAA paper no 2006-3294.